

A Correction Method for Dynamic Model Calculations Using Observational Data and Its Application in Oceanography

K. P. Belyaev^{a, b, d, *}, A. A. Kuleshov^{c, **}, N. P. Tuchkova^b, and C. A. S. Tanajura^d

^a*Shirshov Institute of Oceanology, Russian Academy of Sciences, Moscow, Russia*

^b*Federal Research Center “Computer Science and Control” of Russian Academy of Sciences, Moscow, Russia*

^c*Federal Research Center Keldysh Institute of Applied Mathematics of Russian Academy of Sciences, Moscow, Russia*

^d*Federal University of Bahia, Salvador, Brazil*

**e-mail: kbel55@yahoo.com*

***e-mail: andrew_kuleshov@mail.ru*

Received March 19, 2015

Abstract—A new data assimilation method for the correction of model calculations is developed and applied. The method is based on the least resistance principle and uses the theory of diffusion-type stochastic processes and stochastic differential equations. Application of the method requires solving a system of linear equations that is derived from this principle. The system can be considered as a generalization of the well-known Kalman scheme taking the model’s dynamics into account. The method is applied to the numerical experiments with the HYbrid Coordinate Ocean Model (HYCOM) and Archiving, Validating, and Interpolating Satellite Ocean (AVISO) data for the Atlantic. The skill of the method is assessed using the results of the experiments. The model’s output is compared with the twin experiments, namely, the model calculations without assimilation, which confirms the consistency and robustness of the proposed method.

Keywords: data assimilation methods, path of least resistance principle, ocean dynamics models

DOI: 10.1134/S2070048216040049

1. INTRODUCTION

Data assimilation methods for the observations in the hydrodynamic models of the atmosphere and ocean circulation represent a most interesting and intensively developing area of research in modern computational geophysics. Here the main idea is to combine in the optimal way the model calculations of the fields of the geophysical characteristics (temperature, salinity, pressure, etc.), the field of flow velocities, and other fields with the measurements obtained independently of the model. Such a combination yields new fields of characteristics that are more suitable for further analysis and/or forecasting.

Data assimilation problems arise in modern oceanography, meteorology (weather forecasting), and climatology (forecasting climate fluctuations). The recent achievements in this area are referred in [1–6]. The skill and utility of different data assimilation methods are assessed by comparing the forecast characteristics after assimilation with the control calculations (without assimilation), as well as with the natural observations in an a priori given metric. If the forecast after assimilation appears preferable to its counterpart without assimilation, the corresponding assimilation method can be applied in practice. In addition, it is possible to compare the data assimilation methods by different criteria: the requirements for numerical implementation, their capabilities, computational costs and many other characteristics.

Despite the fact that intensive investigations in this area have been conducted for over 50 years, the ultimate solution of the problem (i.e., the design of a generally accepted best algorithm) is still a major challenge. In some cases, a well substantiated numerical algorithm turns out to be inferior to a simpler empirical algorithm in terms of the forecast accuracy.

There are two basic groups of the mathematical methods used for data assimilation. The first group is based on minimization of a given functional that describes the distance between the model path and the observational data in an appropriate metric. For instance, here we mention the 3D-Var and 4D-Var methods [7, 8]. The second group includes statistical or dynamical-stochastic methods considering the initial problem as one of signal extraction against a noisy background and employing common statistical estima-

tion and/or filtering methods [9–11]. Also, there exist hybrid assimilation methods integrating both these approaches [12, 13].

Data assimilation using the 3D-Var and 4D-Var methods varies the initial condition (the initial field of the parameters) so that the numerical solution path has the shortest distance to the observational data in terms of a given metric. Therefore, variations take place on the whole domain of the model, not locally. According to the alternative approach, i.e., data assimilation using the dynamical-stochastic methods, it is necessary to define a weight matrix that considers the relationships between the observed and calculated values of the parameters. During assimilation, the calculated values vary precisely in the segment of the grid domain with the highest strength of the above relationships; these variations are determined by the covariance between the calculated and observed values at the moment of assimilation. In other words, the variations have a strong localization, being independent of the previous state of the system (the background state), and hence all information on the evolution of the process disappears. However, implementation of the dynamical-stochastic methods is simpler in comparison to the 3D-Var and 4D-Var methods.

The present paper suggests a hybrid assimilation method. Similarly to the dynamical-stochastic schemes, it calculates a certain weight matrix; however, this matrix depends not only on the correlation of the observed and calculated characteristics of the model at a given time but also on the background state. The matrix is derived from the least resistance principle, just as in the 3D-Var and 4D-Var methods. Another feature of the method is that the least action function has a natural form of some limit process in the problem.

As the basic model for data assimilation, we employ version 2.2.14 of the HYbrid Coordinate Ocean Model (HYCOM) [14, 15] configured for the Atlantic in the zone from 79° S to 55° N and from 100° W to 20° E, except the Mediterranean. The model is described in detail below. The numerical experiments also operate the Archiving, Validating, and Interpolating Satellite Ocean (AVISO) data available from www.aviso.altimetry.fr. This work continues the research published in a series of papers [11, 12, 16].

This paper's major goals are given below:

- (a) design, verify, and implement a new data assimilation method;
- (b) demonstrate its representativeness, competitiveness, and applicability in satellite ocean data assimilation;
- (c) study the influence of assimilating satellite ocean data by this method on the other calculated parameters of the model;
- (d) analyze in brief the physical structure of the model's fields before and after assimilation, as well as compare them with the observations.

2. MATHEMATICAL STATEMENT OF PROBLEM

In a certain grid domain, consider a given mathematical model of ocean circulation that is integrated on a finite horizon $[0, T]$. Denote by X the state vector of the ocean, which includes its potential temperature (θ), salinity (S), and sea surface height (SSH). Let N_g and N_{mv} be the number of grid points and the number of model variables, respectively. Therefore, the state vector X has dimensions $N_g \times N_{mv} = r$. Further, designate by Y the vector of observed parameters and by N_o the number of observations each containing N_{ov} independent variables, e.g., θ , and sea surface height anomalies (SSHA) as the differences between SSH and their normal values at the same points. Then the observation vector has dimensions $N_o \times N_{ov} = N$. Generally, $N_{mv} \geq N_{ov}$, since the observations cover only some of the variables calculated in the model. The theory of data assimilation operates two vectors of the ocean's parameters, namely, the ones before and after data assimilation (the background and analysis states X_b, X_a , respectively). They are interconnected by

$$X_a = X_b + K(Y - HX_b). \quad (1)$$

In formula (1), matrix K of dimensions $r \times N$ is the Kalman gain. Matrix H of dimensions $N \times r$ defines an operator projecting the model's space into the observation space. In fact, this operator nullifies the unobserved components of the vector X and performs the linear interpolation of the observed components into the observation points.

Next, a sampling $0 = t_0 < t_1 < \dots < t_N = T, t_{n+1} = t_n + \Delta t$, is made on the horizon $[0, T]$ and the data are assimilated at the moments t_n by formula (1). Consequently, at each moment t_n we have

$$X_{a,n} = X_{b,n} + K_n(Y_n - HX_{b,n}). \quad (2)$$

Let $X_{b,n+1} = F(X_{a,n})$ indicate the model forecast obtained using the background state. Then Eq. (2) takes the form

$$X_{a,n+1} = F(X_{a,n}) + K_{n+1}(Y_{n+1} - HF(X_{a,n})). \tag{3}$$

Assume that the model forecast $F(x)$ represents the antiderivative of some function Λ , i.e.,

$$F(x) = x + \int_{t_n}^{t_{n+1}} \Lambda(x, \tau) d\tau. \tag{4}$$

In this case, Eq. (3) can be rewritten as

$$X_{a,n+1} = X_{a,n} + \int_{t_n}^{t_{n+1}} \Lambda(X_{a,n}, \tau) d\tau + K_{n+1} \left(Y_{n+1} - HX_{a,n} - H \int_{t_n}^{t_{n+1}} \Lambda(X_{a,n}, \tau) d\tau \right). \tag{5}$$

Equation (5) applies to the fields after assimilation, and subscript a will be further omitted.

The earlier works [11, 17] demonstrated that, under definite conditions, the sequence of such processes can be approximated by a stochastic diffusion-type process of the form

$$dX(t) = (I - KH)\Lambda dt + (KQK')dW, \tag{6}$$

where I means the identity matrix and $Q = E(Y - HX)(Y - HX)' + R$ is the sum of the covariance matrix of the modeling error and the covariance matrix R of the instrumental measurement errors. Symbol $'$ stands for transposition of a vector or matrix. By assumption, the matrix R is diagonal; i.e., the values of the instrumental errors have no correlation with each other. Equation (6) also uses the standard notation dW of the Gaussian white noise. The moment t belongs to the interval $t_n < t < t_{n+1}$. In the sequel, all the subscripts are omitted when there is no confusion. As usual, the model is unbiased with respect to the observations, i.e., $E(Y - HX) = 0$, where E signifies the expectation operator (in the physical sense, ensemble averaging). Thus, the observations have zero average deviation from the model results.

The process $X(t)$ is defined at all grid points and for all model variables, see (6). Without loss of generality, suppose that the matrices KH and Q are invertible; i.e., there exist the matrices $(KH)^{-1}$ and Q^{-1} . These conditions imply that the observed and model variables are not linearly expressible via each other. The optimal assimilation problem admits the following statement: find a weight matrix K minimizing the variance of the process $X(t)$ under a given value of its trend. In other words, it is necessary to minimize the matrix KQK' in the sense of some matrix norm under a given value C of the vector $(I - KH)\Lambda$. According to this statement, the vector C is an r -dimensional vector defined at all grid points and having a certain value for each of the model variables.

Prior to the formal solution of the problem, we analyze in brief the physical character of the desired solution. First, expression (6) is a differential equation, and hence the desired solution depends on the initial condition $X(t) = x$ at the moment t , both for a small interval $(t, t + \Delta t)$ and for the whole horizon (t, T) . Matrix Q and vector C must be therefore defined dependent on state x . Second, under $C = \Lambda(x, t)$, the unique solution is the trivial one $K = 0$, which has a physical sense. However, if $C \neq \Lambda(x, t)$, a nontrivial solution always exists, since $\Lambda(x, t) = (KH)^{-1}(\Lambda(x, t) - C)$. Moreover, if C appreciably differs from $\Lambda(x, t)$, then K is very large and the process $X(t)$ in (6) may have a very large diffusion, yielding an unrealistic solution.

Consider the Lagrange functional

$$L(K, \varphi) = \|KQK'\| + \langle \varphi, (I - KH)\Lambda - C \rangle, \tag{7}$$

where φ is the r -dimensional vector of the Lagrange multipliers, and $\|\bullet\|$ denotes some matrix norm.

The vector $(I - KH)\Lambda$ is given, and minimization of the functional $L(K, \varphi)$ is equivalent to minimization of the functional

$$\hat{L}(K, \varphi) = \|KQK' + ((I - KH)\Lambda - C)\varphi\|.$$

Consider the variation of the functional $\hat{L}(K, \varphi)$ in K :

$$\delta \hat{L}(K, \varphi) = \hat{L}(K + \delta K, \varphi) - \hat{L}(K, \varphi),$$

$$\begin{aligned}\hat{L}(K + \delta K, \varphi) &= \|(K + \delta K)Q(K + \delta K)' + [(I - (K + \delta K)H)\Lambda - C]\varphi\| \\ &= \|KQK' + \delta KQK' + KQ\delta K' + \delta KQ\delta K' - \delta KH\Lambda\varphi' + [(I - KH)\Lambda - C]\varphi\|.\end{aligned}$$

Using the symmetry of matrix Q , the identity $KQ\delta K' = \delta KQK'$, and the well-known inequality $\|a\| - \|b\| \leq \|a - b\|$, we obtain the following estimate within the second-order terms:

$$|\delta \hat{L}(K, \varphi)| \leq \|\delta K(2QK' - H\Lambda\varphi')\| = \|(\delta K(2QK' - H\Lambda\varphi'))\|,$$

which gives

$$|\delta \hat{L}(K, \varphi)| \leq \|(2KQ - \varphi(H\Lambda)')\delta K\|. \quad (8)$$

The functional $\hat{L}(K, \varphi)$, and hence the functional $L(K, \varphi)$ defined by (7) achieves its minimum under the zero factor at $\delta K'$ in the right-hand side of (8). In this case, the minimum of $\|KQK'\|$ subject to $(I - KH)\Lambda = C$ is found from the system of equations

$$KQ - \frac{1}{2}\varphi(H\Lambda)' = 0, \quad (9)$$

$$(I - KH)\Lambda = C. \quad (10)$$

Equations (9) and (10) are matrix equations equivalent to $(r + 1) \times N$ scalar equations in the same number of variables. Since the matrix Q is invertible, this system possesses a unique solution, which can be obtained explicitly. Using Eq. (9), we express $K = \varphi(H\Lambda)'Q^{-1}/2$ and substitute into (10) to get

$$\varphi = 2(\Lambda - C)[(H\Lambda)'Q^{-1}H\Lambda]^{-1}.$$

Here the bracketed expression is a number, and the matrix K has the final expression

$$K = \frac{(\Lambda - C)(H\Lambda)'Q^{-1}}{(H\Lambda)'Q^{-1}H\Lambda}. \quad (11)$$

The matrices Q^{-1} and $(H\Lambda)'$ can be canceled only in the one-dimensional case when $r = N = 1$. Then formula (11) becomes the trivial expression $K = (\Lambda - C)/(H\Lambda)$. In the general case, if the component of the drift vector $(I - KH)\Lambda$ is positive, the difference $(Y - HX_b)$ is added to the model forecast (and deduced from it otherwise). This fact has an obvious physical substantiation.

Therefore, the solution of the problem at step $(n + 1)$ is defined by formulas (3) and (11), where vector Λ (see (4)) is calculated using the approximation

$$\Lambda_{n+1} = \frac{F(X_{a,n}) - X_{a,n}}{\Delta t},$$

while the projection operator H and the covariance matrix Q have specific determination in each problem. The method is completely described.

According to the suggested method, calculation of matrix K takes into account the model dynamics $K_{n+1} = K_{n+1}(Y_{n+1}, X_{b,n+1}, X_{a,n})$, in contrast to the classical Kalman filter [10] with $K_{n+1} = K_{n+1}(Y_{n+1}, X_{b,n+1})$.

The method possesses a major advantage that it is possible to find the optimal weight matrix (and thus solve the assimilation problem) with the probability distribution of the deviation from the obtained solution. This distribution satisfies the Fokker–Planck equation [19]

$$\frac{\partial p(t, x)}{\partial t} = -\frac{\partial[(I - KH)\Lambda p(t, x)]}{\partial x} + \frac{1}{2} \frac{\partial^2[(KQK')p(t, x)]}{\partial x^2}, \quad (12)$$

where $p(t, x)$ is the probability density of the random vector $X(t)$. Equation (12) is solved under the initial condition $p(t_0, x) = p_0(x)$ and the boundary condition $p(t, \pm\infty) = 0$, where $p_0(x)$ represents an a priori given function.

3. NUMERICAL EXPERIMENTS AND THEIR RESULTS

The assimilation method has been applied in combination with the HYbrid Coordinate Ocean Model (HYCOM) [20, 21] in its latest version 2.2.14 [22]. In this configuration, the model's grid is located in the Atlantic from Antarctica to 55° north latitude. The model's resolution in the horizontal axis is 0.25° in the east–west direction. The distance between the grid points in the south–north direction varies with the minimum resolution of 0.25° from 10° south latitude to 10° north latitude. In the vertical axis, the model has an isopycnic structure; i.e., the whole ocean from surface to bottom is split into the predetermined levels of the same density (isopycnic lines). The above configuration uses 21 levels. The model resolution in the horizontal axis is 480×760 points. The model calculates 109 independent variables, namely, sea surface height, 3 barotropic variables (the horizontal components of the velocity vector and sea surface pressure), and 5 baroclinic variables for each of the 21 density levels i.e., the horizontal components of the velocity vector, layer thickness, temperature, and salinity. Hence, the state vector X of the model has dimension $r = 480 \times 760 \times 109 = 39763200$. As the observed information, the experiments have employed only the sea surface height anomalies from the AVISO archive. The data have been observed and recorded daily for 8 years from 2002 to 2009. The number of daily observations N varies from 25000 to 30000. The archive also contains the observed levels along the satellite tracks.

Before the numerical experiments on data assimilation, it is necessary to perform several preliminary operations. By assumption, the model is unbiased with respect to the observations, and hence the real average residual (difference) between the model and the observations must be eliminated or at least minimized. For this, we have used a special procedure, i.e., bias elimination along the satellite tracks [16]. The model calculation along each satellite track and the observations are averaged independently along each satellite track (the results of the model calculations are interpolated into the observation points), and then the difference between the average observed value and the average model value on each satellite track is subtracted from the real observation. At the preliminary stage, the observations are also smoothed using the moving average, as the sampling step is approximately 5 km and the grid resolution achieves 25 km. Moreover, inadequate observations and values outside the current zone have been rejected. All these techniques reduce the number of required daily observations by a factor of ten, making N close to 3000.

Specification of the vector C and the covariance matrix Q also runs in part at the preliminary stage. For each grid point in the horizontal plane, it is necessary to draw a circle of radius 0.25° and to average all the observations within the circle; this average is assigned to the grid point under consideration. The value of the vector C at this point is the average minus the model value with assimilation at the previous time step. If the circle contains no observations, the value of the vector C at this point coincides with the model's counterpart. The values of the vectors HF and $H\Lambda$ are defined by analogy. At the same time, matrix Q has a more complicated specification procedure defined by the anomaly strategy, which is common in data assimilation with ensemble interpolation (EnOI). First, it is necessary to calculate spin up 40 years with the external boundary conditions, wind, heat, and moisture flows defined from the NCEP atlas [21]. In this calculation, the daily data for the past 10 years are recorded and averaged over 10 years, and for a specific day the deviation of the calculated value from the obtained average value (the anomaly η) is obtained. This anomaly is interpolated into the observation point using the same scheme as for calculation of vector C : all the anomalies are averaged at the grid points lying within a circle of radius 0.25° near each of the observation points, and the average value is assigned to this observation point. The same technique applies to the state vector x . Next, the covariance matrix Q is calculated by

$$Q = \frac{1}{N_{\text{ens}}} \sum_{i=1}^{N_{\text{ens}}} (\eta_i - x)(\eta_i - x)' + R,$$

where N_{ens} means a given number of ensemble elements (in the experiments, $N_{\text{ens}} = 50$). Matrix R has been described above, and its diagonal contains the values $\delta_{jj} = 0.01 \text{ m}^2$, $j = 1, \dots, N$, as recommended in [22]. To assimilate the data for a specific day, the ensemble elements have been selected around this data within 5 days. For instance, if assimilation is performed for April 7, then the values of the ensemble are defined as April 1, 4, 7, 10, and 13 for these 10 years, i.e., 50 values in total. By this definition, Q represents a symmetric matrix of dimensions $N \times N$, which is invertible as supposed earlier.

Note that specification of matrix Q resembles that of matrix HBH' , where B is the background covariance matrix widespread in Kalman filtering [10]. However, in this case, matrix Q is calculated independently of the state vector x at the previous step (the background state).

Using the developed assimilation method, we have performed numerical experiments on data assimilation in HYCOM. The experiments cover a horizon of 15 days, i.e., $[0, T] = [01.04.2011, 15.04.2011]$, with

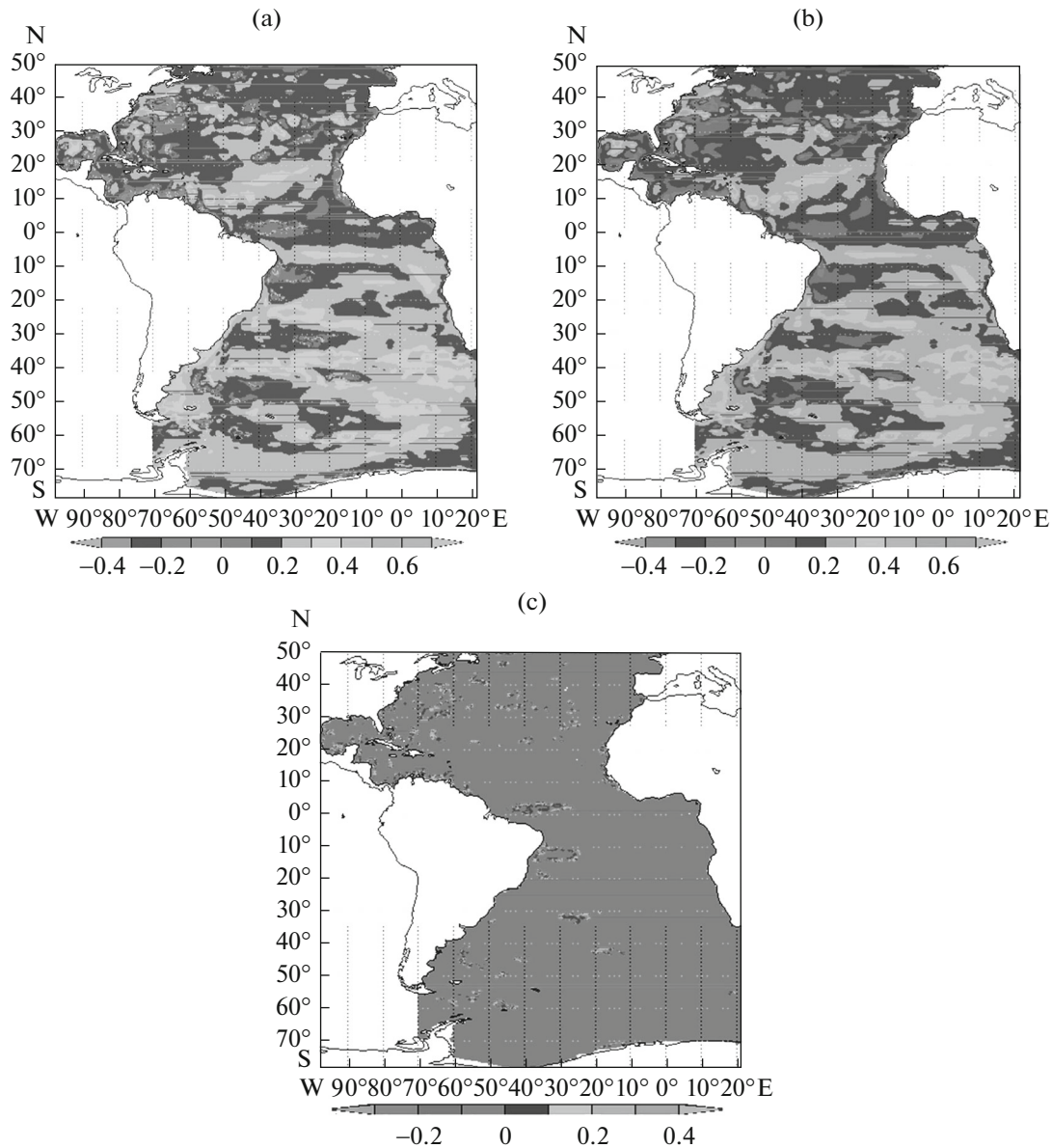


Fig. 1. The SSHA fields (a) after assimilation, (b) before assimilation, and (c) their difference at day 15 (the last day of assimilation).

step $\Delta t = 1$ day, data assimilation at each step by formulas (3) and (11), and specification of vectors Λ , C , HF , and $H\Lambda$, as well as matrix Q , as described above.

For the analysis of the results, it is possible to consider the SSHA field maps obtained before and after assimilation. Figures 1a–1c show the field after assimilation (the analysis field), the field before assimilation (the background field), and their difference for 15 days (the last day of assimilation), respectively. Figure 2 illustrates the SSHA field map yielded by the parallel experiment using the model without assimilation (control calculation) for the same day. As it is clear from Fig. 1a, the SSHA field has an eddy mesogrid structure, which is pronounced in the northern part of the calculation domain (in the Gulf Stream zone), as well as near Drake Strait and the Brazilian–Malvinas border in the southern Atlantic. The amplitudes of the anomalies reach 0.6 m, which is a very large quantity in the synoptic scale. Generally, the fields in Fig. 1b have a similar structure as the field demonstrated in Fig. 1a, but their amplitudes are smaller and the eddy mesogrid dynamics become faint. This is especially noticeable in Fig. 1c, which shows the difference between these fields (the analysis field minus the background field). The northern and southern parts of the Atlantic have explicit eddies with amplitude reaching 0.3 m, both of positive and

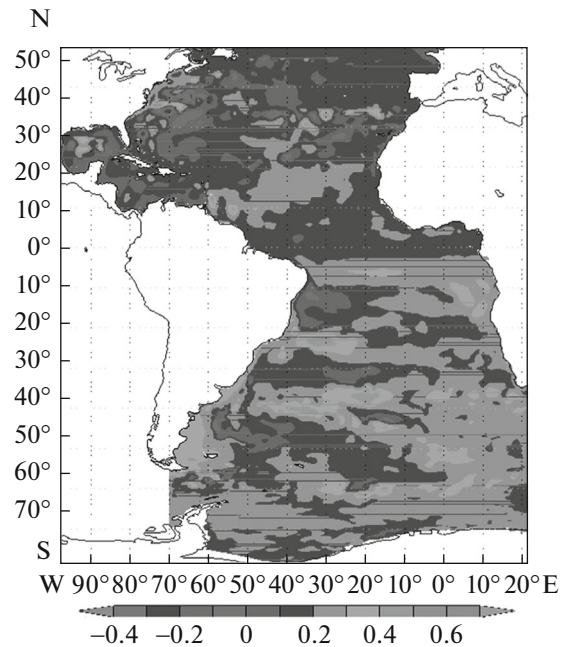


Fig. 2. The SSHA fields for the check calculation.

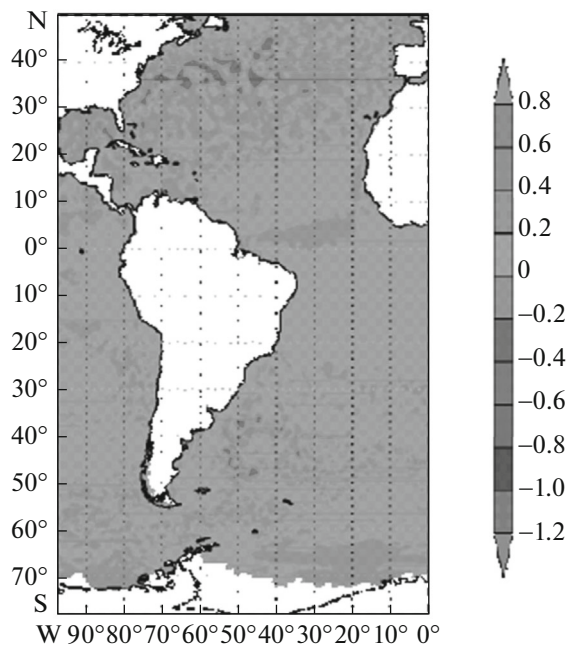


Fig. 3. The interpolated SSHA field and the reanalysis-based observed SSHA field for April 15, 2011.

negative dynamics. Hence, the data assimilation preserves and even strengthens the synoptic and meso-scale structure of the SSHA fields, whereas the model without assimilation smoothens it. This conclusion is verified by the SSHA field obtained using the parallel calculations in the control experiment (see Fig. 2). Here the SSHA field contains appreciably fewer eddies of the synoptic scale and mesoscale and their amplitude is also considerably smaller than in Fig. 1. An exception is the pronounced eddies in the Gulf Stream zone that appear in all the calculations.

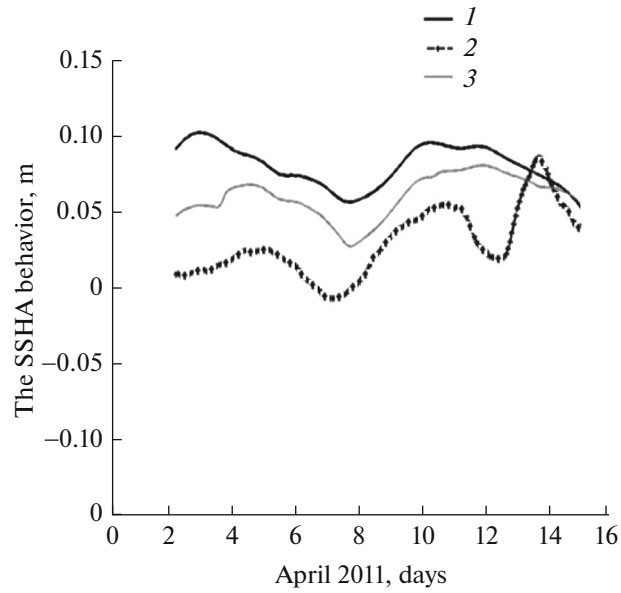


Fig. 4. The SSHA behavior along a satellite track on the model horizon: model calculation without assimilation (curve 1), observed values (curve 2), model calculation with assimilation (curve 3).

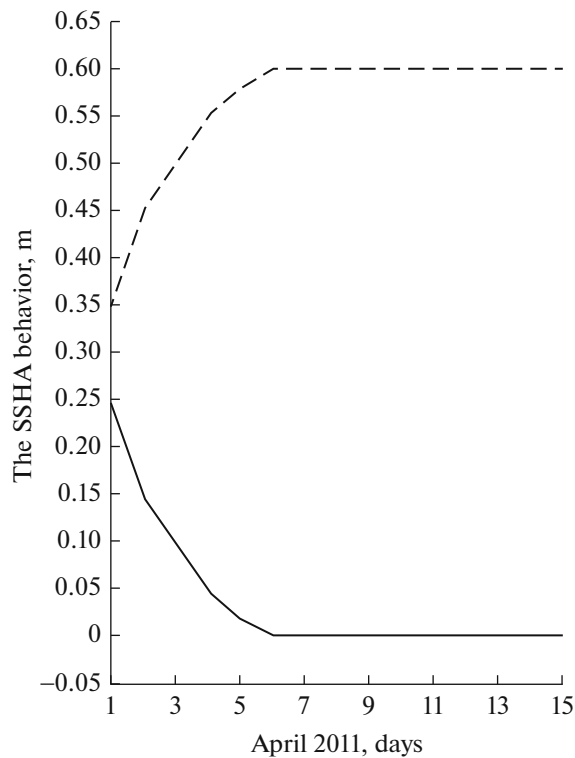


Fig. 5. The bounds of the SSHA analysis field at each point under given initial variance (95% significance level at 40° S, 50° W).

Figure 3 shows the SSHA field for April 15, 2011. This field has been directly copied from the data from www.aviso.altimetry.fr in the NetCDF format and their visualization using the FERRET graphics package. Therefore, the domain in Fig. 3 is not identical to the model domain, see Figs. 1 and 2. Moreover, the quantitative comparison of these fields (the model and observed ones) seems complicated, as the grids do

not coincide and the interpolation procedure yields an additional error that is difficult to consider. However, it is possible to make a qualitative comparison.

According to Fig. 3, the observed field in the equatorial Atlantic is homogeneous, whereas in the northern and southern Atlantic, it has a pronounced eddies structure. The amplitude of these vortices coincides or approaches the SSHA field obtained by data assimilation. Another feature is the existing negative anomaly in the equatorial zone, i.e., a “tongue” along the equator whose amplitude reaches 0.1 m. This anomaly appears in the analysis field (see Fig. 1a), but disappears in the check field; i.e., the model does not reproduce it. The anomaly exists in the field before assimilation, but its amplitude differs from the observations. And we conclude that, due to assimilation, the correction runs properly, both in qualitative and quantitative terms.

The skill of the assimilation methods can be assessed by the closeness of the assimilated field and the observations in comparison to the control field. This technique is widespread, both in the theoretical investigations and practical calculations [1, 17]. Figure 4 shows three curves corresponding to the behavior of the anomalies of the sea surface height along a satellite track during integration of the model, namely, the observed SSHA (dashed curve), the calculated SSHA (thick solid curve), and the assimilated SSHA (thin solid curve). Obviously, the calculated curve lies between the control and observed ones.

At the end of this section, we estimate the adequacy of the obtained curve at a given point during assimilation. As shown above, the assimilation method allows computing the confidence bounds for the constructed analysis field at each point under the given initial variance. Figure 5 presents these bounds with the 95% significance level at 40° S, 50° W. The calculation has been based on the Fokker–Planck equation (12) with the initial Gaussian distribution having a zero mean and 0.01 m² variance. All the parameters of this equation have been defined numerically using the model. We do not describe the calculation method of Eq. (12), as it is similar to the one adopted in [17]. According to Fig. 5, the confidence bounds expand rapidly, becoming almost invariable as of the sixth day of integration. Under the initial anomaly of 0.3 m, the lower bound is close to 0 and the upper one is about 0.6 m.

4. CONCLUSIONS

This paper has been dedicated to the theoretical development and practical implementation of the new data assimilation method based on the theory of diffusion-type random processes.

The method is rather simple to implement and reproduces the real structure of the observed fields at the synoptic scale and mesoscale. It has been demonstrated that, under altimetric data assimilation, the modeling error decreases and the resulting fields are closer to the observed counterparts. Moreover, it is possible to construct the confidence bounds of the modeling error, both in theory and practice.

The paper has analyzed and assimilated only the altimetric fields, more specifically, the anomalies of the sea surface height. However, the method can be used to calculate all the model fields before and after assimilation, as well as to assimilate other observed parameters, particularly, the sea surface temperature and the ARGO drifter data. This is the subject of future research.

ACKNOWLEDGMENTS

The theoretical part of this work, i.e., the development of the new data assimilation method for the correction of model calculations (Section 2), was supported by the Russian Scientific Foundation, project no. 14-11-00434.

REFERENCES

1. M. Ghil and P. Malnotte-Rizzoli, “Data assimilation in meteorology and oceanography,” *Adv. Geophys.* **33**, 141–266 (1991).
2. V. V. Penenko, *Methods of Numerical Modelling of Atmospheric Processes* (Gidrometeoizdat, Leningrad, 1981) [in Russian].
3. G. I. Marchuk and V. V. Penenko, “Application of perturbation theory to problems of simulation of atmospheric processes,” in *Monsoon Dynamics*, Ed. by J. Lighthill and R. Pearce (Cambridge Univ. Press, Cambridge, 1981), pp. 639–655.
4. G. I. Marchuk and V. B. Zalesny, “A numerical technique for geophysical data assimilation problems using Pontryagin’s principle and splitting-up method,” *Russ. J. Numer. Anal. Math. Model.* **8**, 311–326 (1993).
5. V. B. Zalesny and A. S. Rusakov, “Numerical algorithm of data assimilation based on splitting and adjoint equation methods,” *Russ. J. Numer. Anal. Math. Model.* **22**, 199–219 (2007).

6. V. P. Shutyaev and E. I. Parmuzin, "Some algorithms for studying solution sensitivity in the problem of variational assimilation of observation data for a model of ocean thermodynamics," *Russ. J. Numer. Anal. Math. Model.* **24**, 145–160 (2009).
7. V. I. Agoshkov, E. I. Parmuzin, and V. P. Shutyaev, "Observational data assimilation in the problem of Black Sea circulation and sensitivity analysis of its solution," *Izv. Atmos. Ocean. Phys.* **49**, 592–602 (2013).
8. O. Talagrand and P. Courtier, "Variational assimilation of meteorological observations with the adjoint vorticity equation. I: Theory," *Quart. J. R. Meteorol. Soc.* **113**, 1311–1328 (1987).
9. G. Evensen, "Sequential data assimilation with a non-linear quasi-geostrophic model using Monte-Carlo methods to forecast error statistics," *J. Geophys. Res.*, No. 6, 1014–1062 (1994).
10. G. Evensen, "The ensemble Kalman filter: theoretical formulation and practical implementation," *Ocean Dyn.* **53**, 343–367 (2003).
11. K. Belyaev, C. A. S. Tanajura, and J. J. O'Brien, "A data assimilation technique with an ocean circulation model and its application to the tropical Atlantic," *Appl. Math. Model.* **25**, 655–670 (2001).
12. C. A. S. Tanajura and K. Belyaev, "A sequential data assimilation method based on the properties of diffusion-type process," *Appl. Math. Model.* **33**, 2165–2174 (2009).
13. A. C. Lorenc, N. E. Bowler, A. M. Clayton, S. R. Pring, and D. Fairbairn, "Comparison of hybrid-4DVar and hybrid-4DVar data assimilation methods for global NW," *Mon. Wea. Rev.* **143**, 212–229 (2015).
14. R. Bleck and D. B. Boudra, "Initial testing of a numerical ocean circulation model using a hybrid quasi-isopycnal vertical coordinate," *J. Phys. Oceanogr.*, No. 11, 755–770 (1981).
15. R. Bleck, "An oceanic general circulation model framed in hybrid isopycnic–Cartesian coordinates," *Ocean Model.*, No. 4, 55–88 (2002).
16. C. A. S. Tanajura and L. N. Lima, "Assimilation of sea surface height anomalies into hycom with an optimal interpolation scheme over the Atlantic ocean Metarea V," *Geophys. Bras. J.* **31**, 257–270 (2013).
17. K. P. Belyaev, K. A. S. Tanazhura, and N. P. Tuchkova, "Comparison of Argo drifter data assimilation methods for hydrodynamic models," *Oceanology* **52**, 523–615 (2012).
18. F. P. Vasil'ev, *Optimization Methods* (Faktorial, Moscow, 2002) [in Russian].
19. W. M. Wonham, "Stochastic problems in optimal control," in *IEEE International Convention Record* (1963), Pt. 11, pp. 114–124.
20. E. P. Chassignet, H. E. Hurlburt, E. J. Metzger, O. M. Smedstad, J. Cummings, G. R. Halliwell, R. Bleck, R. Baraille, A. J. Wallcraft, and C. Lozano, "US GODAE: Global Ocean Prediction with the HYbrid Coordinate Ocean Model (HYCOM)," *Oceanography* **22**, 64–75 (2009).
21. E. Kalnay et al., "The NCEP/NCAR 40-year reanalysis project," *Bull. Am. Meteorol. Soc.* **77**, 437–472 (1996).
22. J. Xie and J. Zhu, "Ensemble optimal interpolation schemes for assimilating Argo profiles into a hybrid coordinate ocean model," *Ocean Model.* **33**, 283–298 (2010).

Translated by A. Mazurov